Monthly Notices
of the
ROYAL ASTRONOMICAL SOCIETY

MNRAS **488,** 4389–4399 (2019)
Advance Access publication 2019 July 27

doi:10.1093/mnras/stz2036

Dark Energy Survey Year 1 results: the effect of intracluster light on photometric redshifts for weak gravitational lensing

D. Gruen [1,2★†] Y. Zhang [3] A. Palmese [3,4] B. Yanny,[3] V. Busti,[5,6] B. Hoyle,[7,8] P. Melchior,[9] C. J. Miller,[10,11] E. Rozo,[12] E. S. Rykoff,[1,2] T. N. Varga,[7,8] F. B. Abdalla,[4,13] S. Allam,[3] J. Annis,[3] S. Avila,[14] D. Brooks,[4] D. L. Burke,[1,2] A. Carnero Rosell,[6,15] M. Carrasco Kind,[16,17] J. Carretero,[18] R. Cawthon,[19] M. Crocce,[20,21] C. E. Cunha,[1] L. N. da Costa,[6,15] C. Davis,[1] J. De Vicente,[22] S. Desai,[23] H. T. Diehl,[3] J. P. Dietrich,[24,25] A. Drlica-Wagner,[3] B. Flaugher,[3] P. Fosalba,[20,21] J. Frieman,[3,19] J. García-Bellido,[26] E. Gaztanaga,[20,21] D. W. Gerdes,[10,11] R. A. Gruendl,[16,17] J. Gschwend,[6,15] D. L. Hollowood,[27] K. Honscheid,[28,29] D. J. James,[30] T. Jeltema,[27] E. Krause,[31] R. Kron,[3,19] K. Kuehn,[32] N. Kuropatkin,[3] O. Lahav,[4] M. Lima,[5,6] H. Lin,[3] M. A. G. Maia,[6,15] J. L. Marshall,[33] F. Menanteau,[16,17] R. Miquel,[18,34] R. L. C. Ogando,[6,15] A. A. Plazas,[35] A. K. Romer,[36] V. Scarpine,[3] I. Sevilla-Noarbe,[22] M. Smith,[37] M. Soares-Santos,[38] F. Sobreira,[6,39] E. Suchyta,[40] M. E. C. Swanson,[17] G. Tarle,[11] D. Thomas,[14] V. Vikram,[41] and A. R. Walker[42] (DES Collaboration)

Affiliations are listed at the end of the paper

Accepted 2019 July 19. Received 2019 July 18; in original form 2018 September 21

ABSTRACT

We study the effect of diffuse intracluster light on the critical surface mass density estimated from photometric redshifts of lensing source galaxies, and the resulting bias in a weak lensing measurement of galaxy cluster mass. Under conservative assumptions, we find the bias to be negligible for imaging surveys like the Dark Energy Survey with a recommended scale cut of $\geq$200 kpc distance from cluster centres. For significantly deeper lensing source galaxy catalogues from present and future surveys like the Large Synoptic Survey Telescope program, more conservative scale and source magnitude cuts or a correction of the effect may be necessary to achieve percent level lensing measurement accuracy, especially at the massive end of the cluster population.

Key words: gravitational lensing: weak – galaxies: clusters: general – galaxies: distances and redshifts – cosmology: observations.

1 INTRODUCTION

Weak lensing mass calibration is a key to achieving the full potential of galaxy cluster cosmology (for a discussion, see e.g. von der Linden et al. 2014). Numerous lensing studies have provided cluster mass estimates over the last years (e.g. Gruen et al. (e.g. Gruen et al. 2014; von der Linden et al. 2014; Hoekstra et al. 2015; Okabe & Smith 2016; Melchior et al. 2017; Simet et al. 2017; Dietrich et al. 2019; McClintock et al. 2019). The statistical power of such analyses is continuously growing with precise lensing source catalogues around large cluster samples coming from Dark Energy Survey (DES),[1] HSC,[2] and KiDS,[3] and future *Euclid*,[4]

★ E-mail: dgruen@stanford.edu
† Einstein Fellow.

[1] https://www.darkenergysurvey.org
[2] http://hsc.mtk.nao.ac.jp/ssp/
[3] http://kids.strw.leidenuniv.nl/
[4] https://www.euclid-ec.org/

Large Synoptic Survey Telescope (LSST),[5] or *WFIRST*[6] data. This improvement in statistics requires an equivalent push for reducing systematic uncertainties in measurement and modelling of lensing signals. State-of-the-art studies account for systematic effects such as deviations of the assumed model of the cluster matter density profile from the truth (e.g. Becker & Kravtsov 2011), systematics in lensing source catalogues (e.g. Zuntz et al. 2018), excess contamination of the lensing source catalogue with cluster member galaxies (e.g. Melchior et al. 2017; Medezinski et al. 2018), and biases and calibration uncertainties in lensing source photometric redshifts inherent to the algorithms used for estimating them (e.g. Gruen & Brimioulle 2017; Hoyle et al. 2018). In recent studies, each of these effects cause uncertainty on cluster mass at the level of one to a few per cent (e.g. Melchior et al. 2017).

In this paper, we investigate another effect on redshift estimates of weak lensing sources – the bias due to contamination of source photometry from diffuse intracluster light (ICL). In our ICL model, we consider light from the central galaxy and from unbound stars in the cluster potential (see examples of studies or reviews in Zwicky 1951, 1952; Gonzalez, Zabludoff & Zaritsky 2005; Zibetti et al. 2005; Mihos 2015; Kravtsov, Vikhlinin & Meshcheryakov 2018; Montes & Trujillo 2018) as well as the light of faint member galaxies below the survey selection threshold. The diffuse light biases the flux and colour measurements of lensing source galaxies, and causes a systematic change in photometric estimates of their redshift distributions. Among other effects, the spectral energy distribution (SED) of passive stellar populations at the cluster redshift introduces a mild cluster rest-frame D4000 break to the observed SED of the lensing source galaxy. These changes in flux and colour affect the redshift assigned, especially for star-forming galaxies with weaker break features.

Careful analysis of colour–magnitude space could be used to select galaxies less susceptible to these effects, and composite models for blended galaxies could in principle fully account for them. Given the complexity and algorithm dependence of source photometry and redshift estimation, we do not aim to provide a prescription for correcting ICL photo-z contamination in this paper. Our goal is rather to evaluate approximately and, if possible, conservatively, what amplitude of bias we expect and identify the regimes in which it can be ignored.

In Section 2, we describe our model for the surface brightness of ICL, using the results of Zhang et al. (2019). In Section 3, we derive our estimate for how diffuse ICL of given surface brightness biases the lensing amplitude predicted from photometric redshifts, based on Gruen & Brimioulle (2017). Section 4 combines these two components of the model to estimate the bias in lensing excess density profiles in a typical current (DES-like) and future (LSST-like) survey, as a function of cluster redshift and separation from the cluster centre. We conclude the study in Section 5.

Estimates of a quantity q are denoted as $\hat{q}$. All magnitudes given in the $u^\star g' r' i' z'$ bands are in CFHT/Megacam filters[7] u.MP9301, g.MP9401, r.MP9601, i.MP9701, z.MP9801 and AB units until otherwise noted. Surface brightnesses are given in nJy arcsec^{-2} units. These can be converted to counts arcsec^{-2} at a magnitude zero-point of 30 with a conversion factor of 3.63 nJy count^{-1}, i.e. 3.63 nJy arcsec^{-2} correspond to 30 mag arcsec^{-2}. Cosmological distances for the scaling of lensing signal amplitudes are calculated in a flat Λ cold dark matter cosmology with $\Omega_{\rm m,0} = 0.27$, and masses are expressed assuming a Hubble constant $H_0 = 70\,{\rm km\,s^{-1}\,Mpc^{-1}}$.

[5] https://www.lsst.org/
[6] https://wfirst.gsfc.nasa.gov/
[7] http://cfht.hawaii.edu/Instruments/Filters/megaprime.html

2 INTRACLUSTER LIGHT MODEL

The goal of this section is to derive a model for the surface brightness of ICL. We describe it as a function of cluster mass, cluster redshift, and projected physical distance from the cluster centre.

The distribution of ICL is a debated topic in the literature. It is believed that the ICL contains a significant amount of stellar mass (Behroozi, Wechsler & Conroy 2013; Contini et al. 2014; Pillepich et al. 2018), comparable to that of cluster central galaxies or the rest of the cluster galaxies. However, measurements of ICL in various samples (Gonzalez et al. 2005; Zibetti et al. 2005; Krick, Bernstein & Pimbblet 2006; Toledo et al. 2011; Burke et al. 2012; Gonzalez et al. 2013; Montes & Trujillo 2014; DeMaio et al. 2015) do not necessarily find agreement on such a massive component, possibly due to methodological difference (such as differences in filter bands, or surface brightness thresholds and other criteria used to distinguish ICL from galaxies, see e.g. Morishita et al. 2017, Montes & Trujillo 2018 and the discussion in the latter), cluster-to-cluster variations (e.g. Krick & Bernstein 2007), cluster dynamic state (e.g. Jiménez-Teja et al. 2018, 2019), or redshift evolution and the surface brightness limits of ICL (e.g. Burke, Hilton & Collins 2015). By averaging the light profile of ∼300 optically selected clusters, Zhang et al. (2019) quantified the ICL distribution at $z \sim 0.25$ for clusters more massive than $\sim 2 \times 10^{14}\,{\rm M}_\odot$. A comparison of the stellar mass in the ICL component with the total stellar mass in DES Y1 redMaPPer clusters measured in Palmese et al. (2019) shows that the ICL, together with the central galaxy, makes up ∼ 40 per cent of the total cluster stellar mass in the sample from Zhang et al. (2019). We make use of these measurements to model ICL.

There are three components empirically seen as diffuse light in clusters with the methodology of Zhang et al. (2019): pure ICL due to stars not bound to any galaxy, the light of faint cluster members below a detection/masking threshold, and scattered light of the cluster galaxies in the outskirts of the point-spread function (PSF).

We will call the first component, dominant in most regimes, *pure* ICL. Our model for pure ICL is based on the measurements presented in Zhang et al. (2019). In that work, sky brightness around centres of optically selected clusters is measured on co-added images. The latter are made by masking well-detected galaxies ($i < 22.4$) on single-epoch DES images without background subtraction, and combining all frames of the full cluster sample while placing the cluster centre at the centre of the co-add image. Three effects contaminate the light measured such: background contamination due to random field galaxies, light of faint un-masked cluster member galaxies ($i > 22.4$), and light of bright cluster member galaxies escaping the applied masking. These components are estimated and subtracted to yield the measurement of pure ICL.

As an additional contaminant, the PSF effect exists with every ground-based telescope at similar levels (see studies in Moffat 1969; King 1971; Racine 1996; Bernstein 2007; Sandin 2014 and also discussions in Zhang et al. 2019). It is a contaminant to the measurement in Zhang et al. (2019), yet greatly subdominant in the case of the DECam PSF, given that 97 per cent of light is contained within a 5 arcsec radius of the PSF (Zhang et al. 2019, their section 4), and intrinsic ICL is a much larger fraction of total cluster light. We find that the effect of PSF changes the ICL profile by less than 5 per cent in the relevant radial redshift ranges.

Our second term, the amount of light in *undetected* galaxies, depends on the magnitude limit to which cluster members are detected and can be successfully deblended. We approximate this as a fixed limiting magnitude $m^{\rm lim}$.

The full function we are trying to model is thus

$$f_{\rm ICL}(M_{200m}, z_{\rm d}, r, m^{\rm lim}) = f_{\rm pure\ ICL}(M_{200m}, z_{\rm d}, r) + f_{\rm undetected}(M_{200m}, z_{\rm d}, r, m^{\rm lim}) \,, \quad (1)$$

with cluster mass M_{200m}, cluster redshift $z_{\rm d}$, and projected physical distance r from the cluster centre. We describe our model for both terms in the following sections.

2.1 Model for pure ICL

Zhang et al. (2019) have measured the pure ICL profile around a richness-redshift selected sample of redMaPPer clusters in DES Y1 data. In this subsection, we convert their measurement of pure ICL at these fixed parameters into a prediction for $f_{\rm pure\ ICL}(M_{200m}, z_{\rm d}, r)$ based on the assumptions that

(i) The stellar mass density profile is self-similar, i.e. indistinguishable between different clusters when expressed as a function of $r/r_{200m} \propto r \times M_{200m}^{-1/3}$. This is qualitatively consistent with the results of a richness-binned analysis in Zhang et al. (2019).

(ii) ICL has a fixed stellar mass density profile in physical coordinates across redshifts, which leads to a re-scaling of stellar mass per solid angle with the square of angular diameter distance. We note that there is an ongoing debate in the literature about the growth of ICL over cosmic time, which is discussed below.

(iii) ICL is passively evolving. As a function of redshift, it follows the corresponding luminosity evolution.

These three assumptions can be written as the three re-scaling terms on the right-hand side of the expression

$$f^{i'}_{\rm pure\ ICL}(M_{200m}, z_{\rm d}, r) = f^{\rm Zhang}_{\rm ICL}\left(r \times \left(\frac{M_{200m}}{M^{\rm fid}_{200m}}\right)^{-1/3}\right) \times \left(\frac{D_{\rm A}(z_{\rm d})}{D_{\rm A}(z_{\rm fid})}\right)^2 \times 10^{-0.4\left(m_{i',z_{\rm d}} - m_{\rm fid}\right)} \,. \quad (2)$$

Here, $f^{\rm Zhang}_{\rm ICL}(r)$ is the ICL surface brightness of Zhang et al. (2019), measured for a fiducial mass $M^{\rm fid}_{200m} = 3 \times 10^{14}\,{\rm M}_\odot$ and redshift $z_{\rm fid} = 0.25$. $m_{i',z_{\rm d}} - m_{\rm fid}$ is the apparent magnitude difference of a passively evolving galaxy seen at redshift $z_{\rm d}$ in CFHT i' band and at redshift $z_{\rm fid}$ in DES r' band. For the purpose of this paper, we use a Bruzual & Charlot (2003) model with solar metallicity ($Z = 0.02$), no dust, and with star formation beginning 10 Gyr before $z = 0$ and subsequently declining as $e^{-t/\tau}$ with $\tau = 0.1$ Gyr. The ratio of angular diameters $D_{\rm A}$ corrects for the change of angular scale of the ICL profile with redshift.

Examples of ICL profiles transformed in cluster redshift, mass and filter band are shown in Fig. 1. In this figure and all that follows, we apply azimuthal averaging and a smoothing of ± 40 kpc at $r > 150$ kpc to reduce the noise of the pure ICL measurement of Zhang et al. (2019) at large radii.

Note that we assume ICL to not accrete or eject stars over time. It is often argued that ICL forms relatively late, assembling most of its total stellar mass during galaxy interactions after redshift 1.0 (Monaco et al. 2006; Rudick, Mihos & McBride 2006; Conroy, Wechsler & Kravtsov 2007; Burke et al. 2012; Behroozi et al. 2013; Contini et al. 2014; Zhang et al. 2016). Since our model is based on ICL measurements at $z \sim 0.25$, the luminosity of ICL at higher redshift ($z > 0.25$) is likely to be lower than, or at most equal to, the amount predicted from our passive evolution model. Hence, the photometric bias due to ICL at higher redshift ($z > 0.25$) is likely to be less severe than that predicted in the paper. Passive evolution is a conservative assumption for the purpose of estimating photo-z bias.

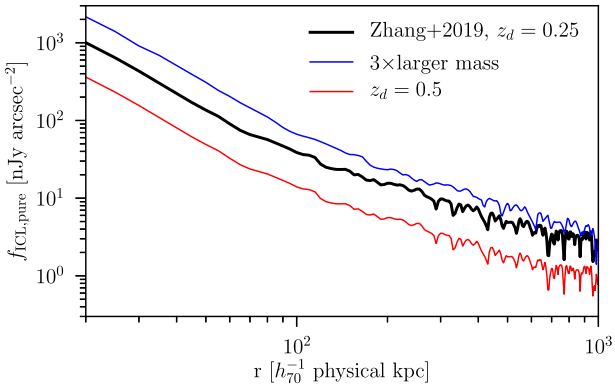

Figure 1. Pure ICL profiles (solid lines) measured in DES (black) and transformed to higher mass (blue) and redshift (red) according to equation (2). Dotted lines show the additional ICL due to undetected cluster members (equation 3) in a survey that detects galaxies down to $r = 22.5$.

Finally, to set the ICL fluxes in other bands, we assume that at any redshift, ICL has the same colour as the passive galaxy population. In reality, ICL could be somewhat bluer in colour, especially at large cluster-centric distance. This is due to its lower metallicity, related to its build-up from tidal stripping of cluster members and disruption of dwarf galaxy members (e.g. Montes & Trujillo 2014; Presotto et al. 2014; DeMaio et al. 2018; Huang et al. 2018; Montes & Trujillo 2018; Contini, Yi & Kang 2019; Zhang et al. 2019). We confirm that an excess in blue light of 0.1 mag in g band, comparable to the colour effect of the expected metallicity offsets, would reduce our predicted bias, yet by less than 5 per cent, at all cluster redshifts studied here.

2.2 ICL from undetected cluster members

The light of undetected member galaxies is an additional contribution to diffuse light in the cluster. To add this to our full ICL model, we use the same methodology as Zhang et al. (2019) apply for *subtracting* the faint galaxy contribution towards a measurement of pure ICL (see their section 5). Namely, we assume that at any radius, the fraction of total cluster member light in faint galaxies is determined by a spatially homogeneous luminosity function. From the measured light in bright cluster members we can then predict the undetected contribution.

Formally, we write

$$f_{\rm undetected}(M_{200m}, z_{\rm d}, r, m^{\rm lim}) = f_{\rm members}(M_{200m}, z_{\rm d}, r) \times S(z_{\rm d}, m^{\rm lim}, \infty), \quad (3)$$

where $S(z_{\rm d}, m^{\rm lim}, \infty)$ is the fraction of the integral over the cluster member luminosity function contributed by the faint end from $m^{\rm lim}$ to ∞.

For a Schechter (1976) luminosity function with faint-end slope α,

$$\frac{{\rm d}N_{\rm gal}}{{\rm d}L} \propto \phi(L) \propto \left(\frac{L}{L^\star}\right)^\alpha \exp[L/L^\star] \,, \quad (4)$$

Table 1. Best-fitting values for equation (7) for the DES r'-band flux from redMaPPer members. The reduced χ^2 is 1.5.

a (nJy arcsec^{-2})	b_r	b_λ	b_z
9.95 ± 0.12	1.205 ± 0.010	-0.831 ± 0.037	8.96 ± 0.10

the integrated luminosity is given by

$$I(L_1, L_2) = \int_{L_1}^{L_2} L\ \phi(L) \mathrm{d}L \propto \left[\Gamma\left(\alpha+2, \frac{L_2}{L^\star}\right) - \Gamma\left(\alpha+2, \frac{L_1}{L^\star}\right)\right], \tag{5}$$

with the incomplete gamma function Γ. In this work, we assume $\alpha = -1$, as motivated by Rykoff et al. (2014), thus

$$S(z_\mathrm{d}, m_1, m_2) = \Gamma\left(1, 10^{0.4(m^\star - m_1)}\right) - \Gamma\left(1, 10^{0.4(m^\star - m_2)}\right). \tag{6}$$

Note that for this luminosity function about 18 per cent of the total flux is contained in galaxies fainter than $0.2L_\star$ and more than 99 per cent of the total flux is contained in members brighter than $m^\star + 5$.

The characteristic magnitude $m^\star$ (Koester et al. 2007; Rykoff et al. 2014) is a function of cluster redshift z_d, which we calculate from the Bruzual & Charlot (2003) model, normalized to match the SDSS DR8 (Aihara et al. 2011) redMaPPer catalogue (Rykoff et al. 2014) at $z = 0.2$.

We approximate f_members from the light of redMaPPer cluster members $f_\mathrm{redMaPPer}$ in the 'flux limited' DES Y1 catalogue (McClintock et al. 2019). RedMaPPer estimates the probability of each galaxy along the line of sight to belong to the red cluster member population above $0.2L_\star$ based on its position relative to the central galaxy and its colour–magnitude relative to the empirically calibrated red sequence at the cluster redshift. The count of these galaxies within a cluster defines the redMaPPer richness λ. They are detected by DES over the full redshift range of the redMaPPer catalogue, allowing us to empirically constrain the evolution of f_members with redshift. However, they are only the bright, red subset of the cluster galaxy population. For f_members in equation (3), we thus use the luminosity function to re-scale $f_\mathrm{redMaPPer}$ by a factor $I(0.2L^\star, \infty)/I(0, \infty) = 1.22$ from equation (5), for the missing members at $L < 0.2L_\star$. In the relevant radial range, these passive galaxies dominate the cluster member population (e.g. Zu & Mandelbaum 2016), which is why we do not correct for the missing non-passive members.

From examining these light profiles, we find that the DES r'-band flux f_members of redMaPPer cluster members approximately follows a power law in projected radial distance, cluster richness and redshift, as

$$f_\mathrm{members}(\lambda, z_\mathrm{d}, r) = a \left(\frac{r}{\tilde{r}}\right)^{-b_r} \left(\frac{\lambda}{\tilde{\lambda}}\right)^{-b_\lambda} \left(\frac{1+z_\mathrm{d}}{1+\tilde{z}_\mathrm{d}}\right)^{-b_z}, \tag{7}$$

where $\tilde{r} = 240$ kpc, $\tilde{\lambda} = 40$, and $\tilde{z}_\mathrm{d} = 0.5$ are the pivot values for richness and cluster redshift, and a and $b_{r/\lambda/z}$ are our fit parameters for overall amplitude and power-law exponents, respectively.

Equation (7) is fit between 20 and 1000 kpc, and the best-fitting results from a χ^2 minimization are given in Table 1 and r is the comoving projected distance from the cluster centre in kpc. The flux used is the SExtractor AUTO measurement in DES r' band (Drlica-Wagner et al. 2018) and this is weighted for each galaxy from the redMaPPer catalogue by the corresponding membership probability. The masked regions are taken into account when computing the flux per area, and the errors on the flux profiles are computed through a jackknife resampling. The bins in richness ($20 < \lambda < 140$) and redshift ($0.1 < z < 0.8$) are chosen to have a similar number of clusters in most bins. To convert $f_\mathrm{members}(\lambda, z_\mathrm{d}, r)$ to $f_\mathrm{members}(M_{200m}, z_\mathrm{d}, r)$ we apply the $\langle \ln\lambda | M_{500c}\rangle$ relation of Saro et al. (2015). We convert between M_{200m} and their M_{500c} using the mass–concentration relation of Duffy et al. (2008). We note that $\langle\lambda|M\rangle \neq e^{\langle \ln\lambda|M\rangle}$ due to intrinsic scatter in λ at fixed M. For the purpose of this paper and consistency with our scaling of the Zhang et al. (2019) model for pure ICL, we set the amplitude of the scaling relation such that $\langle\lambda|M_{200m} = 3\times10^{14}\,\mathrm{M}_\odot, z = 0.25\rangle = 30$.

The m_lim to use with equation (3) is dependent on survey and detection strategy. For the DES Y1 Gold catalogue Drlica-Wagner et al. (2018, their fig. 8), a conservative m_lim for the purpose of estimating the contribution of cluster members to diffuse light is a DES i'-band magnitude of 22.5.

We model the light of undetected members at a given cluster-centric radius as homogeneously distributed, rather than concentrated at the positions of the actual galaxies. If the surface brightness of ICL at the positions of actual undetected galaxies is small enough so that the linearity of photo-z bias found in Section 3.2 holds, the predicted mean bias does not depend on this assumption of homogeneity. For member galaxies with larger surface brightness, non-linear blending effects will likely play a role – we consider these to be an issue separate to the ICL studied in this paper.

We note that the contribution of undetected cluster members becomes important at large cluster mass, high redshift, and for a shallow survey (see dotted lines in Fig. 1). For our DES parameters, it contributes the majority of ICL for a cluster of $M_{200m}/M_\odot = 10^{15}$ at $z_\mathrm{d} > 0.6$. For lower mass or redshift in DES, it is a subdominant component – contributing, in the relevant regimes, between 10 and 40 per cent of ICL. For LSST it is negligible due to the completeness down to fainter magnitudes.

3 LENSING PHOTO-z BIASES FROM DIFFUSE LIGHT

The goal of this section is to derive a model for the bias in the lensing measurement of cluster surface matter density due to leakage of ICL into lensing source galaxy photometry used for estimating source redshift (z_s) distributions. The source redshift-dependent quantity needed for lensing measurements of a matter distribution at redshift z_d is the predicted amplitude of the lensing signal. This amplitude is proportional to

$$\beta = D_\mathrm{ds}/D_\mathrm{s}, \tag{8}$$

the ratio of angular diameter distances between lens and source D_ds and to the source D_s, defined as the ratios of physical to angular sizes of objects at z_s seen by observers at z_d and 0, respectively. The true value of β could be calculated if redshifts were known for sources and lenses. In practice, the source redshift distributions are estimated from their photometry. Any bias in photo-z thus manifests as a bias in the amplitude $\hat{\beta}$ estimated from them. In this work, we therefore primarily consider biases in $\hat{\beta}$, rather than in the redshift distribution more generally.

We define this bias as

$$\left(\hat{\beta}/\beta\right) - 1 \approx F(f_\mathrm{ICL}, z_\mathrm{d}, \text{source magnitude limit}), \tag{9}$$

where f_ICL is the surface brightness of ICL present at the position of the lensing source galaxy in question and z_d is the redshift of the lens. F is the model for the ICL-related bias we derive in this section. The larger the statistical power of a lensing survey, the

smaller a bias can be tolerated before it significantly affects the analysis. Current (and future) surveys aim for multiplicative biases to be below the few (to one) per cent level.

In the remainder of this section we describe the basic lensing formalism, followed by our framework for estimating the impact of ICL on empirical redshift estimates in Section 3.1. We then develop the right-hand side of equation (9) in Section 3.2. In this, $f_{\rm ICL}$ is denoting the level of ICL surface brightness at the position of the lensing source population – the model for $f_{\rm ICL}$ as a function of cluster mass, redshift, and distance from the cluster centre was presented in Section 2.

The image of a lensing source (or ensemble of sources) located on some annulus around a gravitational lens at angular diameter distance $D_{\rm d}$ from the observer is subject to tangential gravitational shear (e.g. Bartelmann & Schneider 2001, for a review)

$$\gamma_t = \Sigma_{\rm crit}^{-1} \times \Delta\Sigma = \frac{4\pi G D_{\rm d}}{c^2} \times \beta \times \Delta\Sigma \ . \tag{10}$$

The excess surface density $\Delta\Sigma$ at radius r is the difference of the mean mass per area *inside* and *on the edge* of a circle of radius r,

$$\Delta\Sigma(r) = \langle\Sigma(<r)\rangle - \Sigma(r) \ . \tag{11}$$

$\hat{\beta}$ can be estimated from the photo-z redshift probability density $\hat{p}(z)$ as

$$\hat{\beta} = \int \hat{p}(z) \frac{D_{\rm ds}(z_{\rm d}, z)}{D_{\rm s}(z)} \, {\rm d}z \ . \tag{12}$$

For the mean shear signal of an ensemble of lensing source galaxies i, each with weight w_i, this can be written as

$$\hat{\beta} = \frac{\sum_i w_i \times \hat{\beta}_i}{\sum_i w_i} \ , \tag{13}$$

where w_i is a source weight and $\hat{\beta}_i$ the estimated β of source i from equation (12). For the optimal (minimum variance) estimator of mean shear or surface mass overdensity, $w_i \propto \beta_i/\sigma^2_{{\rm e},i}$, or, in practice, $\propto \hat{\beta}_i/\sigma^2_{{\rm e},i}$ where $\sigma^2_{\rm e}$ is the shape noise variance including intrinsic and measurement noise.

In the case of an unbiased estimate $\hat{\beta}$, this connects mean tangential shear $\langle\gamma_{\rm t}\rangle$ and excess surface mass density $\Delta\Sigma$ as

$$\langle\gamma_{\rm t}\rangle = \frac{\sum_i w_i \times \gamma_{{\rm t},i}}{\sum_i w_i} = \frac{4\pi G D_{\rm d}}{c^2} \times \hat{\beta} \times \Delta\Sigma. \tag{14}$$

Thus, for example, if $\hat{\beta}$ is biased low, e.g. due to a bias in photo-z, the estimated $\Delta\Sigma$ is biased high, and vice versa. This is the source of bias we evaluate in the following. For an indirect impact of the bias in photometric redshifts via the estimation of cluster member contamination of the lensing source sample, see Appendix A.

3.1 Framework for empirical redshift estimation

Our framework for estimating the effect of ICL on photo-z is a simple empirical method that gives an unbiased estimate of $p(z|\boldsymbol{m})$, where $\boldsymbol{m}$ is a vector of colours and magnitude. The accuracy of its redshift distribution estimates are limited only by selection effects or sample variance of the available reference sample with known redshifts. In this work, we use the same sample for reference and bias determination, which cancels these effects: without ICL, the redshift distribution recovery is perfect by construction. Given this, and a model for the colour of and total flux from diffuse light that enters each source, we can estimate how much the $\hat{\beta}$ of equation (13) will be biased. We use this simple empirical method as a proxy for any photometric redshift estimation that could be performed using similar wide-band survey data, e.g. from DES or, with the caveat that the fainter magnitude limit is not fully covered by our CFHT-based reference catalogues, LSST.

The empirical method is a simple decision tree described in detail in Gruen & Brimioulle (2017) and publicly available at https://github.com/danielgruen/betatree/. Given a complete reference sample of galaxies with photometric measurements in a set of bands and with known true redshift, the decision tree provides an unbiased and close to optimal estimate of $p(z)$ based on the colour–magnitude information in any subset of these bands. The method splits the colour–magnitude space spanned by the subset of bands into hyper-rectangles (leaves of the decision tree), and assigns to each galaxy as its $p(z)$ the histogram of true redshifts of reference galaxies in that leaf. We make the simplifying assumption that the lensing source sample is a magnitude limited sample of galaxies, i.e. ignore additional explicit or implicit selections on pre-seeing size, shape or profile that are commonly present in such catalogues. For the purpose of these tests, and because no sufficiently faint magnitude limited sample of galaxies with spectroscopic z is available, we use the same photo-z sample and (unless otherwise noted) the same settings of the tree as in Gruen & Brimioulle (2017). The galaxies used are measured from the Canada–France–Hawaii Telescope Legacy Survey (CFHTLS) Deep fields, four fields with 1 deg^2 area each, for which 8-band photometry from CFHTLS and the WIRCam Deep Survey is available. The sample is complete to $i' \approx 25$, although we use a shallower magnitude limited sample for all analyses to follow. The combination of high signal-to-noise photometry for magnitude limits relevant for lensing source samples and large volume relative to e.g. the COSMOS field make the sample well suited for our purpose.

Operationally, we estimate the bias of photo-z due to ICL with the following procedures.

(i) Build a decision tree from magnitude limited sample $20 \leq i' \leq 24$ (23.5, 24.5 as variants), optimized for a cluster redshift $z_{\rm d}$, from $g'r'i'z'$ (also $u^\star g'r'i'z'$ as a variant) colour–magnitude information. The magnitude limits are chosen to approximately match present and future samples of lensing source galaxies (e.g. Mandelbaum et al. 2018; Zuntz et al. 2018)

(ii) Estimate $\hat{\beta}$ in each leaf of the decision tree as the mean of β_i of all reference galaxies in that leaf.

(iii) Determine the ICL $X - i'$ colour c_X as the median of the $X - i'$ colour of all galaxies in the reference catalogues with $z \in [z_{\rm d} - 0.02, z_{\rm d} + 0.02]$ and a best-fitting SED of a passive galaxy, where X is one of $(u^\star)g'r'z'$. Note that this assumes that the ICL has the same SED as a red galaxy: this condition is satisfied in the clusters studied in Zhang et al. (2019), where the ICL colours are consistent with those from redMaPPer (Rykoff et al. 2014) centrals within the inner 10 kpc, becoming bluer in the outer regions but still consistent with the red sequence galaxy population. Likewise, DeMaio et al. (2018) found that ICL colours are consistent with red sequence galaxies over a wider redshift range ($0.29 < z < 0.89$) using HST imaging.

(iv) Generate ICL-contaminated fluxes of each reference galaxy as $f_X^{\rm cont.} = f_X + \mu_A \times A \times f_{{\rm ICL},i} \times 10^{-0.4 c_X}$. In this, A is defined to be the area of a circle with the post-seeing half-light radius of the galaxy. In our tests, we homogenized the data to a seeing half-light radius of 0.4 arcsec to make this independent of the observing conditions of the CFHTLS-Deep fields. The factor μ_A accounts for the effective sensitivity of a method of measuring galaxy fluxes to diffuse light. We note that μ_A will depend strongly on the method used for extracting fluxes. By running SExtractor in dual-image

mode with a detection image contaminated with diffuse flux, we find $\mu_A = 2.5$ for DETMODEL model-fitting fluxes. DETMODEL fluxes are derived by fitting PSF convolved Sersic profile models to the galaxy images in a cut-out region. In our configuration, we follow the DES convention of fitting a PSF-convolved single exponential profile to the galaxies (Drlica-Wagner et al. 2018). The value of $\mu_A = 2.5$ is thus what we use in the following analysis.[8]

(v) Re-assign reference galaxies to leaves of the tree generated in (i), based on the contaminated colour–magnitude information.

(vi) Estimate biased mean $\hat{\beta}$ for the contaminated case as the lensing-weighted mean (i.e. with weight $w \propto \hat{\beta}$ of the leaf a galaxy falls into) of the respective $\hat{\beta}$ for each galaxy as determined in (ii) .

(vii) Estimate unbiased mean β by weighting galaxies by their biased $\hat{\beta}$ as in (vi), but using their true reference redshifts to determine the β to average.

The ratio of the $\hat{\beta}$ of step (vi) and the unbiased true β of step (vii), minus 1, is the bias we are trying to determine. Note that at $f_{\rm ICL} = 0$, the two are, by construction, identical. In other words, the decision tree is an unbiased β estimator unless the sample is affected by photometric biases or selection effects.

3.2 Model

In this section, we apply the scheme laid out in Section 3.1 to derive an expression for the bias in $\Delta\Sigma$ as a function of ICL surface brightness, lens redshift, and magnitude limit of the source sample (equation 9).

Judging from the surface brightness of ICL observed in Zhang et al. (2019), the relevant range is $f_{\rm ICL} < 40$ nJy arcsec^{-2} (>27.4 mag arcsec^{-2}) as observed outside ≈100 kpc. In this range and given the sizes and magnitudes of lensing source galaxies,[9] ICL is a perturbation on top of the galaxies' intrinsic flux, such that we can attempt to approximate the effect of ICL on photo-z as linear. We study the linearity of biases in $\hat{\beta}$ at a range of lens redshifts $z_{\rm d} = 0.2$–0.8 in steps of 0.1 and limiting magnitudes of the source sample $m_{\rm lim} \in \{23.5, 24.0, 24.5\}$. Fig. 2 shows selected results for illustration that the bias is indeed well approximated as linear in $f_{\rm ICL}$ for the most relevant regimes. Only for the highest redshift clusters are non-linear effects visible at larger ICL flux levels. This is potentially related to the fact that the relevant source populations that are lensed by the cluster are located at high redshift. Their characteristic apparent magnitude is thus relatively faint and more susceptible to change due to ICL leakage. In the following, we will assume the bias on $\hat{\beta}$ due to ICL is linear in ICL flux, and use the measurement at $f_{\rm ICL} = 14$ nJy arcsec^{-2} (4 counts per arcsec^{-2} at ZP = 30) to determine the slope. This choice is a trade-off: the added flux due to ICL is large enough to allow a high signal-to-noise measurement of the bias, but small enough that it does not suffer from non-linear effects or lead to problems due to sources that are below the $m < 25.5$ limit of the CFHTLS-Deep catalogue being boosted above the $m_{\rm lim} = 23.5$–24.5 magnitude limit of our source sample.

[8]In AUTO photometry, regardless of the explicit background subtraction settings, SExtractor measures and subtracts a background flux estimate locally. In this mode, it is hence insensitive to a diffuse background, i.e. $\mu_A^{\rm AUTO} = 0$. There are other reasons, in particular the sensitivity to different PSF in different bands, that make AUTO photometry problematic for accurate multiband flux measurements in photometric surveys.

[9]Note that an $i' = 24.5$ galaxy has a flux of 575 nJy, spread out over few arcsec^2.

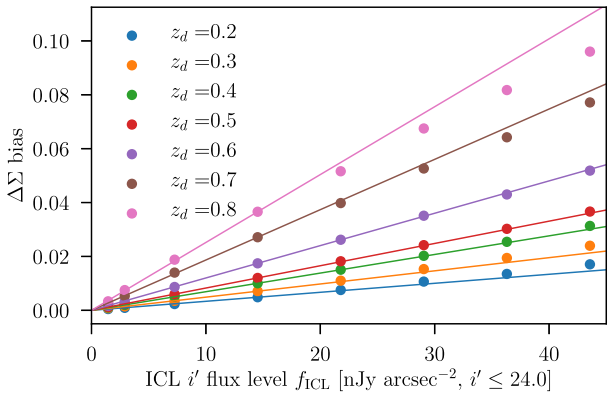

Figure 2. Bias in $\Delta\Sigma$ (defined as the negative of the bias in $\hat{\beta}$) from $g'r'i'z'$ photo-z bias for a sample of source galaxies at $20 \leq i' \leq 24$. Differently coloured lines and points show results for different lens redshifts. 3.63 nJy arcsec^{-2} correspond to 30 mag arcsec^{-2}.

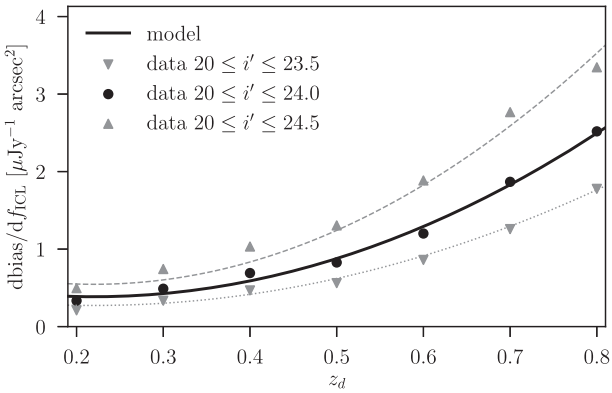

Figure 3. Slope of $\Delta\Sigma$ bias with ICL surface brightness as a function of lens redshift. Circle symbols show measurements made as in Fig. 2, upward and downward triangles the same measurements, but for deeper and shallower source samples. Solid line shows a quadratic model fit at the fiducial magnitude limit, dashed and dotted lines are the same model re-scaled by $2^{m_{\rm lim}-24}$, where $m_{\rm lim}$ is the limiting magnitude of the sample.

For a given source magnitude limit, the slope of bias with ICL surface brightness is a function of lens redshift. By measuring the slope at a range of redshifts, we empirically find that it can be described well, within the range of $z_{\rm d} = 0.2$–0.8, by a quadratic function of $z_{\rm d}$. Measurements and quadratic model (circles and solid line) are shown in Fig. 3.

In addition, we empirically find that a re-scaling of the model by $2^{m_{\rm lim}-24}$ describes the measurements reasonably well at magnitude limits in the range $m_{\rm lim} \in (23.5, 24.5)$ (downward and upward triangles with model as dotted and dashed curve in Fig. 3). The following is the proposed model, for $g'r'i'z'$, fitted from in $z_d \in (0.2, 0.8)$, $m_{\rm lim} \in (23.5, 24.5)$,

$$\frac{{\rm d}(\hat{\beta}/\beta)}{{\rm d}f_{\rm ICL}} \times [\mu{\rm Jy\ arcsec^{-2}}] \approx \left(2.5z_{\rm d}^2 - 1.1z_{\rm d} + 0.028\right) \times 2^{m_{\rm lim}-24}\,. \tag{15}$$

Repeating the same analysis including $u^\star$ band gives a somewhat smaller amplitude of $(1.2z_{\rm d}^2 - 0.063z_{\rm d} + 0.10)$, to be re-scaled the same way as a function of magnitude limit.

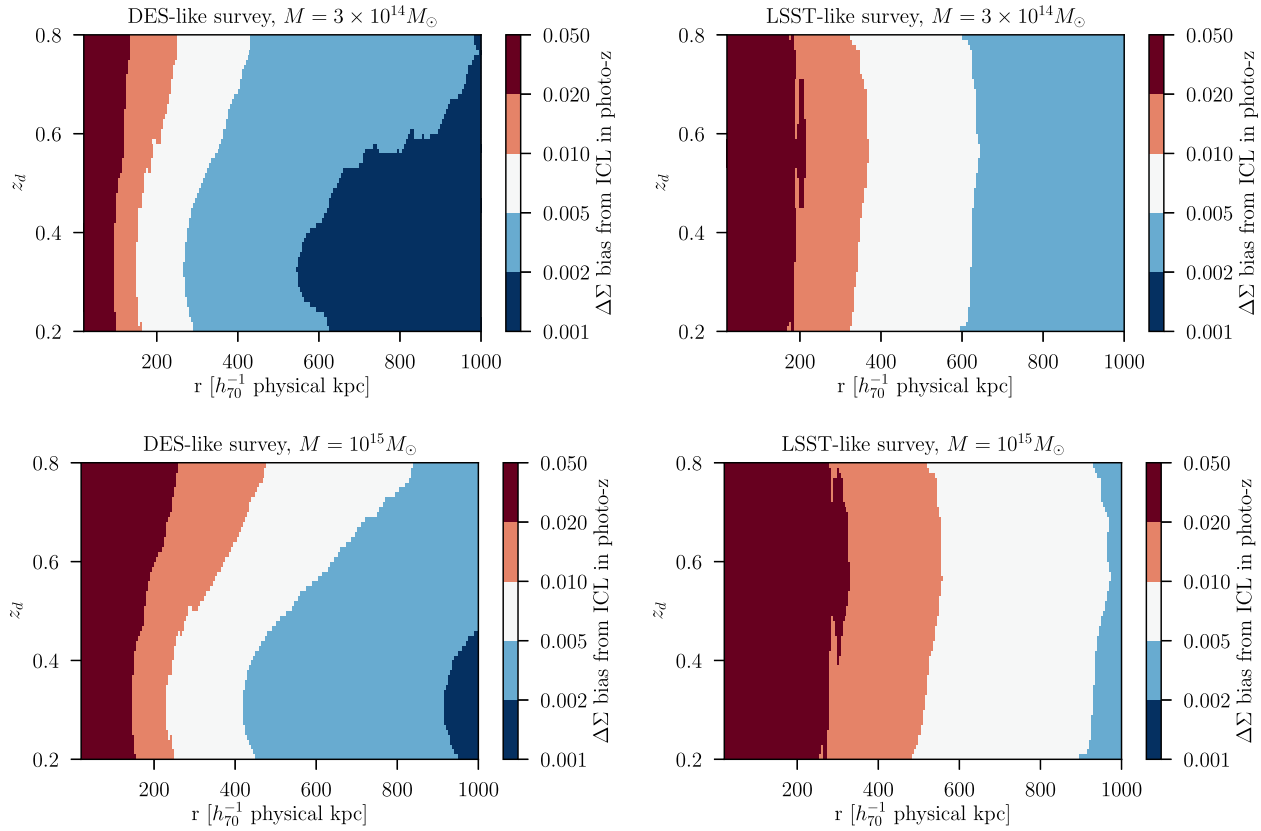

Figure 4. Predictions for the bias in $\Delta\Sigma$ profiles due to ICL-related source photo-z bias for a DES-like (left-hand panels) and LSST-like (right-hand panels) survey, and a cluster of $M_{200m}/M_\odot = 3 \times 10^{14}$ (top) and 10^{15} (bottom). The smallest scales (e.g. $r < 200\,h_{70}^{-1}$ kpc in McClintock et al. 2019) that are most heavily affected by ICL are commonly excised from cluster lensing analyses for other reasons.

4 BIAS PREDICTIONS

Using the models described in Sections 2 and 3, we study the bias in $\Delta\Sigma$ profiles due to contamination of source photometry with diffuse light around clusters.

Due to the dependence on cluster member detection limit of the ICL model (Section 2), and the dependence on source population of the bias per unit ICL flux (Section 3), we need to define a limiting magnitude for the lensing source catalogue and for the detection of cluster members in a given survey. This, in addition to the mass and redshift of a cluster sample, determines our model prediction for ICL related photo-z bias via equations (15) and (1).

We study two cases, and again choose conservative limits (i.e. faint limiting magnitudes for the lensing source catalogue and conservative thresholds for complete cluster member detection): (1) an ongoing *griz* wide-area survey, similar to DES, with lensing sources measured down to $r \approx 23.5$ (Zuntz et al. 2018) and cluster members completely detected and deblended down to $r \approx 22.5$ (Drlica-Wagner et al. 2018) and (2) an ongoing or future deep wide-area *ugriz* survey, similar to HSC or LSST, with lensing sources measured and cluster members completely detected and deblended down to $r \approx 25$.

Results for both cases are shown in Fig. 4, for clusters of two different masses approximately spanning the range currently used for optical cluster cosmology with redMaPPer. These should be compared to the statistical uncertainties of present and future surveys (currently of the order of a few percent, optimistically of the order of 1 per cent) for a sense of whether the biases are relevant.

We find that for a DES-like survey, even under the conservative assumptions made above, the $\Delta\Sigma$ signal estimated outside 200 kpc radius is biased mostly below the 1 per cent level, and only in extreme cases above the 2 per cent level, even for very massive and high-redshift clusters. This implies that at the scale cuts and uncertainties of present DES cluster lensing studies (McClintock et al. 2019), ICL-related photo-z bias is highly subdominant compared to the 5 per cent combined statistical and systematic uncertainty.

For a significantly deeper survey like LSST, biases at the level of 2 per cent are possible on the small to intermediate scales of 200–300 kpc that we hope to use for cluster lensing purposes. This is driven by the larger biases incurred by the fainter sources measured in these surveys. The availability of u-band information in addition to *griz* somewhat alleviates the effect. Given the conservative assumptions made in our study, it is conceivable that the actual bias is only a fraction from our model prediction. But at least for the massive end of the clusters studied with these surveys, diffuse light photo-z contamination requires either more detailed investigation or more conservative cuts in radius or limiting source magnitude.

4.1 Limitations of our model

In the context of these predictions, we summarize the simplifications made in our model, and their likely effect on the bias in practical applications.

Simplifications, i.e. assumptions we had to make due to limited understanding of physical or algorithmic details:

(i) **Generic photo-z algorithm:** For the purpose of this test, we used a simple empirical photo-z algorithm. Assuming that all photo-z algorithms estimate the same relation of multiband flux and redshift, results for other algorithms would likely be similar, yet not equal. We have made simplified tests using BPZ (Benítez 2000; Hoyle et al. 2018) that indicate that this is indeed the case.

(ii) **Leakage of ICL into galaxy photometry:** We assumed leakage to be proportional to a circular aperture with the post-seeing half-light radius of the galaxy. This is an approximation of how a matched aperture or, equivalently, model fitting algorithm for photometric measurements might perform. While we match the leakage scale in this work to the mean observed change in SExtractor DETMODEL flux, other photometry measurement algorithms might show very different results, and galaxy morphology might affect the leakage scale in a galaxy type and redshift-dependent way. Also, small-scale background subtraction could greatly reduce (or even invert) the effect. It is advisable that the leakage of diffuse light into galaxy photometry is estimated from image simulations for any lensing analysis that aims at a percent level accuracy.

(iii) **Linearity of β bias as a function of ICL flux:** Our model assumes that the change in estimated lensing amplitude $\hat{\beta}$ is linear in the ICL surface brightness. While this is appropriate for the relevant range of mean ICL surface brightness, inhomogeneity (i.e. due to undetected yet localized cluster members) could affect the photo-z more or less than predicted here. At the level of deblending possible with present and future lensing surveys, we expect this effect to be subdominant.

(iv) **Pure red cluster member population:** We have assumed that the cluster galaxy population only contains passive galaxies, similar in colour to the ones identified by the redMaPPer algorithm. In practice, clusters contain star-forming galaxies, especially at lower mass and higher redshift. The light of the undetected members among them is likely to have a similar, but not quite equal, effect on photo-z bias as the light of red members. On the radial scales considered here, star-forming members are, however, not a majority of the population. In addition, the light of undetected cluster members is a subdominant component relative to pure ICL, hence we do not expect this assumption to significantly change our conclusions.

(v) **Self-similar scaling of pure ICL:** We have assumed that pure ICL scales self-similarly with cluster mass, i.e. its surface brightness is fixed at a given projected r/r_{500}. While this is consistent with simple comparisons made in Zhang et al. (2019), a more detailed study could reveal deviations.

Conservative assumptions, i.e. ways in which we likely overestimate the effect of ICL in practice:

(i) **Passive SED of ICL:** We assume ICL to share the colour of passive galaxies at the cluster redshift. A population of younger stars in the ICL would likely reduce its effect on photo-z bias due to its similarity in colour to lensing sources at higher redshift. We find that predicted bias is reduced, yet by less than 5 per cent, if ICL should be brighter in g band by 0.1mag, which is approximately the level expected from reduced metallicity.

(ii) **Lack of ICL growth**: We fix the ICL surface density to a measurement at low redshift and predict the expected bias at higher redshift without accounting for any growth of ICL from early to late times. If ICL is assembled over time we thus overestimate biases for higher redshift clusters.

(iii) **Conservative deblending limits:** For DES, we have assumed cluster members to be deblended and thus not affecting source photo-z down to a magnitude limit of $r = 22.5$. At this level, DES Y1 is highly complete – a significant fraction of cluster members below this limit are likely deblended successfully and, unlike assumed, do not in fact contribute to diffuse ICL. As a result, we likely overestimate the associated photo-z bias in DES, in particular at large cluster mass and redshift.

(iv) **Magnitude limited source sample:** We used a simple magnitude cut to define our source sample. Realistic lensing source samples have additional selection criteria. A choice of limiting magnitude at the faint end of the population that is used in a given analysis allows for a conservative prediction of potential biases. For DES Y1/Y3 data, this was possible to do in this work.

Limitations, i.e. regimes in which our model is not reliable:

(i) **Faint limit of source sample:** For LSST data, sufficiently faint reference samples of galaxies with known redshift and flux measurements do not exist to extend the modelling beyond $i' \approx 25$. Assuming that fainter lensing samples are used, the bias derived here is an underestimate of the bias encountered by such analyses.

(ii) **Blending with cluster members:** We only attempt to model diffuse ICL leaking into source photometry at a subdominant level. For the effect of blending between similarly bright cluster member and lensing source galaxies, the model developed here is not applicable. Besides, the success of correctly treating these cases will likely strongly depend on the choice of deblending algorithm.

5 CONCLUSIONS

We have developed a model for the bias in weak lensing estimates of cluster surface mass overdensity due to the contamination of lensed galaxy photometry from diffuse ICL. The latter systematically changes the flux, colour, and thus photometric redshift estimate of the faint galaxies used as lensing sources.

Our model for diffuse light in clusters is simplistic yet conservative for the purpose of this exercise: a pure component of ICL due to un-bound stars in the cluster potential, measured at low redshift (Zhang et al. 2019) and re-scaled in mass and redshift by assuming self-similarity and passive evolution; and a component due to stars in undetected, faint cluster members, extrapolated from detected galaxies by means of the luminosity function. The effect of this surface brightness on photo-z is estimated from an idealized empirical photo-z estimation scheme (Gruen & Brimioulle 2017).

We find that for a DES-like cluster lensing experiment, i.e. with cluster masses up to $M_{200m} = 10^{15}\,\mathrm{M}_\odot$, detection and deblending of cluster members brighter than $i' = 22.5$, and a source sample no fainter than $i' = 23.5$, ICL-related photo-z bias does not significantly affect weak lensing mass reconstruction. Outside a cluster-centric radius of 200 kpc, which is commonly excluded in lensing studies for other reasons, biases are typically below 1 per cent for an M_{200m} $3 \times 10^{14}\,\mathrm{M}_\odot$ cluster, and below 2 per cent at M_{200m} $10^{15}\,\mathrm{M}_\odot$, even under the conservative assumptions we make. The effect of ICL on measured galaxy shapes may well be larger than that, and should be tested with dedicated image simulations.

Deeper source catalogues will be somewhat more susceptible to ICL-related photo-z biases because the flux and colour of faint source galaxies can be changed more strongly by ICL contamination. For massive clusters, lensing source catalogues down to $i' = 25$ show 1 per cent biases at approximately twice the radius as the above DES-like survey. Even fainter sources will likely show even stronger effects, although this is difficult to quantify at present due to the lack of reliable colour–magnitude-redshift information for such samples. An explicit treatment of measured fluxes as a composite of intracluster and lensing source galaxy light in photo-z

estimation could in principle remedy this effect. With moderately conservative scale and magnitude cuts, however, ICL bias of photo-z will be a non-issue even in the next generation of surveys – and with a less conservative examination of the effect, these could likely be moderately relaxed from the recommendations given in this work.

ACKNOWLEDGEMENTS

Support for DG was provided by NASA through the Einstein Fellowship Program, grant PF5-160138 and by Chandra Award Number GO8-19101A, issued by the Chandra X-ray Observatory Center. This work was supported in part by the U.S. Department of Energy under contract number DE-AC02-76SF00515.

The authors thank Fabrice Brimioulle for providing the CFHTLS Deep photometry and photo-z catalogues used in this work. This work has been promoted by fruitful discussions during the workshop series 'Becoming a One-Percenter'.

Funding for the DES Projects has been provided by the U.S. Department of Energy, the U.S. National Science Foundation, the Ministry of Science and Education of Spain, the Science and Technology Facilities Council of the United Kingdom, the Higher Education Funding Council for England, the National Center for Supercomputing Applications at the University of Illinois at Urbana-Champaign, the Kavli Institute of Cosmological Physics at the University of Chicago, the Center for Cosmology and Astro-Particle Physics at the Ohio State University, the Mitchell Institute for Fundamental Physics and Astronomy at Texas A&M University, Financiadora de Estudos e Projetos, Fundação Carlos Chagas Filho de Amparo à Pesquisa do Estado do Rio de Janeiro, Conselho Nacional de Desenvolvimento Científico e Tecnológico and the Ministério da Ciência, Tecnologia e Inovação, the Deutsche Forschungsgemeinschaft, and the Collaborating Institutions in the Dark Energy Survey.

The Collaborating Institutions are Argonne National Laboratory, the University of California at Santa Cruz, the University of Cambridge, Centro de Investigaciones Energéticas, Medioambientales y Tecnológicas-Madrid, the University of Chicago, University College London, the DES-Brazil Consortium, the University of Edinburgh, the Eidgenössische Technische Hochschule (ETH) Zürich, Fermi National Accelerator Laboratory, the University of Illinois at Urbana-Champaign, the Institut de Ciències de l'Espai (IEEC/CSIC), the Institut de Física d'Altes Energies, Lawrence Berkeley National Laboratory, the Ludwig-Maximilians Universität München and the associated Excellence Cluster Universe, the University of Michigan, the National Optical Astronomy Observatory, the University of Nottingham, The Ohio State University, the University of Pennsylvania, the University of Portsmouth, SLAC National Accelerator Laboratory, Stanford University, the University of Sussex, Texas A&M University, and the OzDES Membership Consortium.

This study is based in part on observations at Cerro Tololo Inter-American Observatory, National Optical Astronomy Observatory, which is operated by the Association of Universities for Research in Astronomy (AURA) under a cooperative agreement with the National Science Foundation.

The DES data management system is supported by the National Science Foundation under grant numbers AST-1138766 and AST-1536171. The DES participants from Spanish institutions are partially supported by MINECO under grants AYA2015-71825, ESP2015-66861, FPA2015-68048, SEV-2016-0588, SEV-2016-0597, and MDM-2015-0509, some of which include ERDF funds from the European Union. IFAE is partially funded by the CERCA program of the Generalitat de Catalunya. Research leading to these results has received funding from the European Research Council under the European Union's Seventh Framework Program (FP7/2007–2013) including ERC grant agreements 240672, 291329, and 306478. We acknowledge support from the Australian Research Council Centre of Excellence for All-sky Astrophysics (CAASTRO) through project number CE110001020, and the Brazilian Instituto Nacional de Ciência e Tecnologia (INCT) e-Universe (⟨0:funding-source ⟩CNPq⟨/0:funding-source⟩ grant 465376/2014-2).

This manuscript has been authored by Fermi Research Alliance, LLC under Contract No. DE-AC02-07CH11359 with the U.S. Department of Energy, Office of Science, Office of High Energy Physics. The United States Government retains and the publisher, by accepting the article for publication, acknowledges that the United States Government retains a non-exclusive, paid-up, irrevocable, world-wide license to publish or reproduce the published form of this manuscript, or allow others to do so, for United States Government purposes.

This work is based in part on observations obtained with MegaPrime/MegaCam, a joint project of CFHT and CEA/IRFU, at the Canada-–France–Hawaii Telescope (CFHT) which is operated by the National Research Council (NRC) of Canada, the Institut National des Science de l'Univers of the Centre National de la Recherche Scientifique (CNRS) of France, and the University of Hawaii. This is also based in part on data products produced at Terapix available at the Canadian Astronomy Data Centre as part of the CFHTLS, a collaborative project of NRC and CNRS.

This paper has gone through internal review by the DES collaboration.

REFERENCES

Aihara H. et al., 2011, ApJS, 193, 29
Bartelmann M., Schneider P., 2001, Phys. Rep., 340, 291
Becker M. R., Kravtsov A. V., 2011, ApJ, 740, 25
Behroozi P. S., Wechsler R. H., Conroy C., 2013, ApJ, 770, 57
Benítez N., 2000, ApJ, 536, 571
Bernstein R. A., 2007, ApJ, 666, 663
Bruzual G., Charlot S., 2003, MNRAS, 344, 1000
Burke C., Collins C. A., Stott J. P., Hilton M., 2012, MNRAS, 425, 2058
Burke C., Hilton M., Collins C., 2015, MNRAS, 449, 2353
Chang C. et al., 2018, ApJ, 864, 83
Conroy C., Wechsler R. H., Kravtsov A. V., 2007, ApJ, 668, 826
Contini E., De Lucia G., Villalobos Á., Borgani S., 2014, MNRAS, 437, 3787
Contini E., Yi S. K., Kang X., 2019, ApJ, 871, 24
DeMaio T., Gonzalez A. H., Zabludoff A., Zaritsky D., Bradač M., 2015, MNRAS, 448, 1162
DeMaio T., Gonzalez A. H., Zabludoff A., Zaritsky D., Connor T., Donahue M., Mulchaey J. S., 2018, MNRAS, 474, 3009
Dietrich J. P. et al., 2019, MNRAS, 483, 2871
Drlica-Wagner A. et al., 2018, ApJS, 235, 33
Duffy A. R., Schaye J., Kay S. T., Dalla Vecchia C., 2008, MNRAS, 390, L64
Gonzalez A. H., Zabludoff A. I., Zaritsky D., 2005, ApJ, 618, 195
Gonzalez A. H., Sivanandam S., Zabludoff A. I., Zaritsky D., 2013, ApJ, 778, 14
Gruen D., Brimioulle F., 2017, MNRAS, 468, 769
Gruen D. et al., 2014, MNRAS, 442, 1507
Hoekstra H., Herbonnet R., Muzzin A., Babul A., Mahdavi A., Viola M., Cacciato M., 2015, MNRAS, 449, 685
Hoyle B. et al., 2018, MNRAS, 478, 592

Huang S., Leauthaud A., Greene J. E., Bundy K., Lin Y.-T., Tanaka M., Miyazaki S., Komiyama Y., 2018, MNRAS, 475, 3348
Jiménez-Teja Y. et al., 2018, ApJ, 857, 79
Jiménez-Teja Y. et al., 2019, A&A, 622, A183
King I. R., 1971, PASP, 83, 199
Koester B. P. et al., 2007, ApJ, 660, 221
Kravtsov A. V., Vikhlinin A. A., Meshcheryakov A. V., 2018, Astron. Lett., 44, 8
Krick J. E., Bernstein R. A., 2007, AJ, 134, 466
Krick J. E., Bernstein R. A., Pimbblet K. A., 2006, AJ, 131, 168
Mandelbaum R. et al., 2018, PASJ, 70, S25
McClintock T. et al., 2019, MNRAS, 482, 1352
Medezinski E. et al., 2018, PASJ, 70, 30
Melchior P. et al., 2017, MNRAS, 469, 4899
Mihos C., 2015, IAU General Assembly, 22, 2247903
Moffat A. F. J., 1969, A&A, 3, 455
Monaco P., Murante G., Borgani S., Fontanot F., 2006, ApJ, 652, L89
Montes M., Trujillo I., 2014, ApJ, 794, 137
Montes M., Trujillo I., 2018, MNRAS, 474, 917
Morishita T., Abramson L. E., Treu T., Schmidt K. B., Vulcani B., Wang X., 2017, ApJ, 846, 139
Okabe N., Smith G. P., 2016, MNRAS, 461, 3794
Palmese A. et al., 2019, preprint (arXiv:1903.08813)
Pillepich A. et al., 2018, MNRAS, 475, 648
Presotto V. et al., 2014, A&A, 565, A126
Racine R., 1996, PASP, 108, 699
Rudick C. S., Mihos J. C., McBride C., 2006, ApJ, 648, 936
Rykoff E. S. et al., 2014, ApJ, 785, 104
Sandin C., 2014, A&A, 567, A97
Saro A. et al., 2015, MNRAS, 454, 2305
Schechter P., 1976, ApJ, 203, 297
Sheldon E. S. et al., 2004, AJ, 127, 2544
Simet M., McClintock T., Mandelbaum R., Rozo E., Rykoff E., Sheldon E., Wechsler R. H., 2017, MNRAS, 466, 3103
Stern C. et al., 2019, MNRAS, 485, 69
Toledo I., Melnick J., Selman F., Quintana H., Giraud E., Zelaya P., 2011, MNRAS, 414, 602
Varga T. N. et al., 2018, preprint (arXiv:1812.05116)
von der Linden A. et al., 2014, MNRAS, 443, 1973
Zhang Y. et al., 2016, ApJ, 816, 98
Zhang Y. et al., 2019, ApJ, 874, 165
Zibetti S., White S. D. M., Schneider D. P., Brinkmann J., 2005, MNRAS, 358, 949
Zu Y., Mandelbaum R., 2016, MNRAS, 457, 4360
Zuntz J. et al., 2018, MNRAS, 481, 1149
Zwicky F., 1951, PASP, 63, 61
Zwicky F., 1952, PASP, 64, 242

APPENDIX A: EFFECT OF ICL ON BOOST FACTOR ESTIMATES

Leakage of cluster members into the lensing source sample, i.e. the erroneous use of cluster members as putative background galaxies, is a well-known cause for systematic error in cluster lensing. Because cluster members are not gravitationally lensed regardless of their estimated redshift, this reduces the amplitude of the measured shear signal relative to a model prediction. Many analyses, especially those suffering from relatively poor photometric information that does not allow a pure selection of lensing sources at $z > z_{\rm cl}$ without great losses in sample size, have used a radially dependent *boost factor* correction (Sheldon et al. 2004). That is, they divided the measured signal (or multiplied the model prediction) by a factor equal to the fraction of lensing weight actually due to non-member galaxies (e.g. Melchior et al. 2017; McClintock et al. 2019).

The quantity needed for this correction is the fraction of lensing weight due to cluster members $f_{\rm cl}$ in each radial bin. This has often been estimated from the clustering of lensing sources with the lens positions. The blending of sources with large, bright cluster member galaxies is a known contaminant that is, however, difficult to quantify and correct without full re-processing of the survey with artificially injected faint galaxy images.

A different way of finding $f_{\rm cl}$ is based on the decomposition of the estimated, lensing weighted $p_{\rm est}(z)$ into a component measured in non-cluster fields $p_{\rm field}(z)$ and a component with different shape due to contaminating cluster members $p_{\rm member}(z)$, as

$$p_{\rm est}(z) = (1 - f_{\rm cl}) \times p_{\rm field}(z) + f_{\rm cl} \times p_{\rm member}(z) \; . \tag{A1}$$

This method, developed in a series of papers (Gruen et al. 2014; Melchior et al. 2017; Varga et al. 2018) and applied in several other works (Chang et al. 2018; Medezinski et al. 2018; Dietrich et al. 2019; Stern et al. 2019) has the advantage that it is at first order insensitive to blending. It is, however, potentially susceptible to photo-z biases and source redshift-dependent selection effects in the vicinity of the cluster (see also the note in Medezinski et al. 2018, their section 6.2).

We test the effect of ICL leakage into photometry on boost factors estimated with equation (A1). Specifically, we use the scheme implemented in Melchior et al. (2017) and McClintock et al. (2019) and validated in Varga et al. (2018) to check the methodology of these studies in the presence of ICL. Here, $p_{\rm member}$ is assumed to be a Gaussian distribution. Its mean and width are varied, alongside $f_{\rm cl}$, to find the best-fitting boost factor in a least-squared metric between the left-hand and right-hand side of equation (A1).

We simulate the presence of a member population of a cluster at redshift $z_{\rm d}$ by mixing the redshift distribution of a magnitude limited sample of $i' < 23.5$ with a Gaussian of mean $z_{\rm d} + 0.1$ and width $\sigma_z = 0.1$.

For true contaminations $f_{\rm cl} = 0.1$, 0.2, 0.4 and lens redshifts between $z_{\rm d} \in [0.2, 0.6]$, common for the settings in Melchior et al. (2017) and McClintock et al. (2019), the maximum bias introduced by ICL in our model at $f_{\rm ICL} = 15$nJ arcsec^{-2} is $\Delta f_{\rm cl} = 0.008$, or

$$\frac{{\rm d}\, f_{\rm cl}}{{\rm d}\, f_{\rm ICL}} \lesssim 0.0005 \; . \tag{A2}$$

This is to be interpreted as a multiplicative bias on $\Delta\Sigma$ and significantly smaller than the effect on β shown in Fig. 2. Where the latter is negligible, ICL does therefore not significantly impact boost factors estimated from $p(z)$ decomposition.

[1]*Kavli Institute for Particle Astrophysics & Cosmology, P. O. Box 2450, Stanford University, Stanford, CA 94305, USA*
[2]*SLAC National Accelerator Laboratory, Menlo Park, CA 94025, USA*
[3]*Fermi National Accelerator Laboratory, P. O. Box 500, Batavia, IL 60510, USA*
[4]*Department of Physics & Astronomy, University College London, Gower Street, London, WC1E 6BT, UK*
[5]*Departamento de Física Matemática, Instituto de Física, Universidade de São Paulo, CP 66318, São Paulo 05314-970, SP, Brazil*
[6]*Laboratório Interinstitucional de e-Astronomia – LIneA, Rua Gal. José Cristino 77, Rio de Janeiro, RJ 20921-400, Brazil*
[7]*Max Planck Institute for Extraterrestrial Physics, Giessenbachstrasse, D-85748 Garching, Germany*
[8]*Fakultät für Physik, Universitäts-Sternwarte, Ludwig-Maximilians Universität München, Scheinerstr 1, D-81679 München, Germany*
[9]*Department of Astrophysical Sciences, Princeton University, Peyton Hall, Princeton, NJ 08544, USA*
[10]*Department of Astronomy, University of Michigan, Ann Arbor, MI 48109, USA*
[11]*Department of Physics, University of Michigan, Ann Arbor, MI 48109, USA*

[12]*Department of Physics, University of Arizona, Tucson, AZ 85721, USA*
[13]*Department of Physics and Electronics, Rhodes University, PO Box 94, Grahamstown 6140, South Africa*
[14]*Institute of Cosmology & Gravitation, University of Portsmouth, Portsmouth PO1 3FX, UK*
[15]*Observatório Nacional, Rua Gal. José Cristino 77, Rio de Janeiro, RJ 20921-400, Brazil*
[16]*Department of Astronomy, University of Illinois at Urbana-Champaign, 1002 W. Green Street, Urbana, IL 61801, USA*
[17]*National Center for Supercomputing Applications, 1205 West Clark St., Urbana, IL 61801, USA*
[18]*Institut de Física d'Altes Energies (IFAE), The Barcelona Institute of Science and Technology, Campus UAB, E-08193 Bellaterra (Barcelona), Spain*
[19]*Kavli Institute for Cosmological Physics, University of Chicago, Chicago, IL 60637, USA*
[20]*Institut d'Estudis Espacials de Catalunya (IEEC), E-08193 Barcelona, Spain*
[21]*Institute of Space Sciences (ICE, CSIC), Campus UAB, Carrer de Can Magrans, s/n, E-08193 Barcelona, Spain*
[22]*Centro de Investigaciones Energéticas, Medioambientales y Tecnológicas (CIEMAT), Avda. Complutense, 40, E-28040 Madrid, Spain*
[23]*Department of Physics, IIT Hyderabad, Kandi, Telangana 502285, India*
[24]*Excellence Cluster Universe, Boltzmannstr 2, D-85748 Garching, Germany*
[25]*Faculty of Physics, Ludwig-Maximilians-Universität, Scheinerstr 1, D-81679 Munich, Germany*
[26]*Instituto de Fisica Teorica UAM/CSIC, Universidad Autonoma de Madrid, E-28049 Madrid, Spain*
[27]*Santa Cruz Institute for Particle Physics, Santa Cruz, CA 95064, USA*
[28]*Center for Cosmology and Astro-Particle Physics, The Ohio State University, Columbus, OH 43210, USA*
[29]*Department of Physics, The Ohio State University, Columbus, OH 43210, USA*
[30]*Harvard-Smithsonian Center for Astrophysics, Cambridge, MA 02138, USA*
[31]*Department of Astronomy/Steward Observatory, 933 North Cherry Avenue, Tucson, AZ 85721-0065, USA*
[32]*Australian Astronomical Observatory, North Ryde, NSW 2113, Australia*
[33]*Department of Physics and Astronomy, George P. and Cynthia Woods Mitchell Institute for Fundamental Physics and Astronomy, Texas A&M University, College Station, TX 77843, USA*
[34]*Institució Catalana de Recerca i Estudis Avançats, E-08010 Barcelona, Spain*
[35]*Jet Propulsion Laboratory, California Institute of Technology, 4800 Oak Grove Dr., Pasadena, CA 91109, USA*
[36]*Department of Physics and Astronomy, Pevensey Building, University of Sussex, Brighton BN1 9QH, UK*
[37]*School of Physics and Astronomy, University of Southampton, Southampton SO17 1BJ, UK*
[38]*Physics Department, Brandeis University, 415 South Street, Waltham, MA 02453, USA*
[39]*Instituto de Física Gleb Wataghin, Universidade Estadual de Campinas, 13083-859 Campinas, SP, Brazil*
[40]*Computer Science and Mathematics Division, Oak Ridge National Laboratory, Oak Ridge, TN 37831, USA*
[41]*Argonne National Laboratory, 9700 South Cass Avenue, Lemont, IL 60439, USA*
[42]*Cerro Tololo Inter-American Observatory, National Optical Astronomy Observatory, Casilla 603, La Serena, Chile*

This paper has been typeset from a TEX/LATEX file prepared by the author.